

# Validation of Turbulence Models through the Study of Incompressible Flow past a NACA 0012 Airfoil

Guruprasad M. Godbole<sup>#1</sup>

<sup>#</sup>Department of Mechanical Engineering, Sinhgad College of Engineering, Pune, India

**Abstract**— In this paper, Computational Fluid Dynamics (CFD) analysis of two-dimensional (2D) incompressible flow past a NACA 0012 airfoil at Reynolds number of  $6 \times 10^6$  for different angles of attack has been presented. In order to validate the turbulence models by comparison with experimental data, the simulations were performed by solving the steady-state governing equations of continuity and momentum conservation, together with one of the three turbulence models, viz. Spalart-Allmaras, Realizable  $k-\varepsilon$  and  $k-\omega$  Shear Stress Transport (SST). The flow domain was divided into approximately 84,000 cells, with a greater resolution in the near-wall region of the airfoil for better accuracy. The free-stream velocity was constant while the analysis was performed for three different angles of attack,  $0^\circ$ ,  $10^\circ$  and  $15^\circ$ . The computed values of lift coefficient and drag coefficient were found to have good agreement with the experimental data.

**Keywords**— CFD, NACA 0012 airfoil, turbulence models, Spalart-Allmaras, Realizable  $k-\varepsilon$ ,  $k-\omega$  SST, lift coefficient, drag coefficient

## I. INTRODUCTION

An airfoil is a streamlined shape or surface such that useful motion (lift) is produced by the air moving around it. [1] The cross-section of an airplane wing is an airfoil. Airfoils are also used in applications such as horizontal and vertical axis wind turbines. Thus, the study of the flow around an airfoil in order to determine the aerodynamic characteristics, such as lift and drag coefficients is of paramount importance. The most common way of studying the air flow around the airfoil by experimental methods is testing the airfoil in a wind tunnel. However, actual testing of airfoils may not be possible every time due to various reasons such as the lack of a wind tunnel testing facility. In such cases, it is a common practice to employ Computational Fluid Dynamics (CFD) techniques in order to simulate and study the flow of air around the airfoil. CFD is popularly used in the design, analysis and optimization of equipment associated with aerodynamics.

The National Advisory Committee for Aeronautics (NACA) 0012 airfoil is a well-documented 4-digit series airfoil. The first and the second digits indicate the maximum camber and the location of maximum camber respectively, as a percentage of chord length. The last two digits indicate the maximum thickness of the airfoil as a percentage of chord length. The first two digits of the NACA 0012 airfoil are both 0, because the airfoil is symmetric, i.e it has no camber. 12 indicates that the maximum thickness of the NACA 0012 airfoil is 12% of the total chord length. The NACA 0012 airfoil has been used in the B-17 Flying Fortress and Cessna 152 as well as in the helicopter Sikorsky S-61 SH-3 Sea King. [2]

The very first step in the simulations is the creation of the geometry, followed by meshing of the domain, which is one of the most important aspects of the problem. The accuracy of the solution directly depends on the quality of the mesh. Once the mesh is generated, the boundary conditions can be applied and the governing equations, together with one of the turbulence models can be solved. The numerical solution is obtained, examined and compared with the available experimental data.

The present analysis aimed at validating the turbulence models by evaluating the flow around the NACA 0012 airfoil. The turbulence models which have been considered are the Spalart-Allmaras model, the Realizable  $k-\varepsilon$  model and the  $k-\omega$  Shear Stress Transport (SST) model.

## II. LITERATURE REVIEW

Sadikin *et al.* [3] have presented a CFD simulation of air flow past a 2D NACA 0012 airfoil at Reynolds number  $3.0 \times 10^6$ , and at angles of attack from  $-10^\circ$  to  $15^\circ$ . The fluid flow around the airfoil was studied by solving the steady state governing equations of continuity and momentum conservation combined with one of Spalart-Allmaras, Realizable  $k-\varepsilon$  and the  $k-\omega$  Shear Stress Transport (SST) models. It was observed that the Realizable  $k-\varepsilon$  model eliminated the small separation bubble on the upper surface of the airfoil and delayed the separation flow. The lift and drag coefficients investigated were found to have good agreement with other published data.

Eleni *et al.* [2] have analysed the 2D subsonic flow over a NACA 0012 airfoil operating at a Reynolds number of  $3 \times 10^6$  at different angles of attack. The flow was obtained by solving steady state governing equations of continuity and momentum conservation together with one of the three [Spalart-Allmaras, Realizable  $k-\varepsilon$  and the  $k-\omega$  Shear Stress Transport (SST)] turbulence models. The analysis aimed to

validate the models by comparison of the predictions with experimental values, to show the behaviour of the airfoil at the given conditions and to establish a verified method of solution. Two areas in CFD that require further work were observed, i.e. transition point prediction and turbulence modeling.

Ahmed *et al.* [4] have validated the analysis of 2D flow over the NACA 0012 airfoil with NASA Langley Research Center validation cases. To predict the flow accurately, the  $k-\omega$  Shear Stress Transport (SST) turbulence model was utilized with turbulence intensity 1% at the velocity inlet and 5% at the pressure outlet. This validated simulation technique was then utilized to analyse the aerodynamic characteristics of a plain flapped NACA 0012 airfoil subjected to various flap angles and Mach numbers.

### III. METHODOLOGY

In this study, the 2D CFD analysis was performed in ANSYS Fluent for incompressible flow at Reynolds number  $6 \times 10^6$  with chord length 1 m, and compared with experimental results for different values of angle of attack ' $\alpha$ ' ( $0^\circ$ ,  $10^\circ$  and  $15^\circ$ ). In order to validate the simulation, the operating and boundary conditions are matched with those of NASA Langley Research Center validation cases. [5]

#### A. Domain Meshing

The size of the mesh is crucial in order to generate an accurate solution. As a greater number of nodes are used, the solution tends to become more accurate, however, increasing the number of nodes also means an increase in the required computer memory and time for computation. Therefore, it is necessary to estimate an appropriate number of nodes to obtain a sufficiently accurate numerical solution.

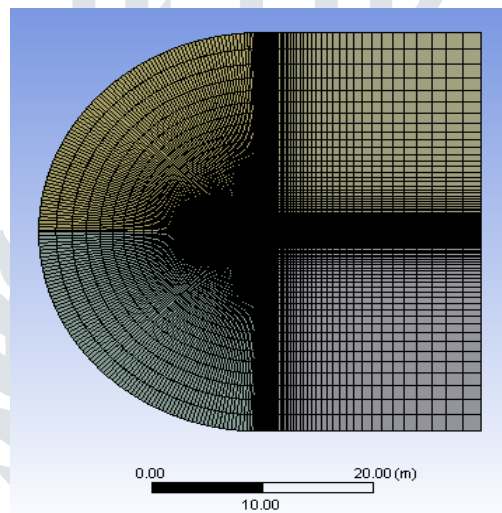


Fig. 1 C-type grid topology

According to [2], a C-type grid topology with approximately 80,000 cells is sufficient to generate an accurate grid-independent result. Hence a similar topology with approximately 84,000 cells was employed. The mesh was highly resolved near the airfoil surface in order to correctly capture the boundary layer. The domain height was set to 20 times the chord length and the height of the first cell adjoining the surface of the airfoil was set to  $10^{-5}$ , which gives a value of  $y^+$  that is sufficient to adequately resolve the inner part of the boundary layer.

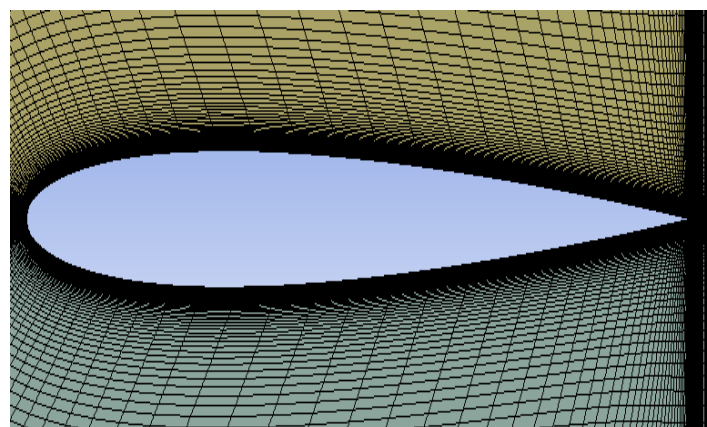


Fig. 2 Near-wall mesh resolution

### B. Boundary Conditions and Solution

The steady state governing equations of continuity and momentum conservation were solved coupled with one of Spalart-Allmaras, Realizable  $k-\varepsilon$  and  $k-\omega$  Shear Stress Transport (SST) turbulence models. After the domain was meshed, the required turbulence model was selected and the boundary conditions were applied. The inlet boundary condition was set to velocity inlet whereas the outlet boundary condition was set to pressure outlet. The recommended default values of Turbulent Intensity and Turbulent Viscosity Ratio were used for both the inlet and outlet boundary conditions. The airfoil was set to the no-slip condition.

Before computing the solution, the residuals of continuity and the variables were set to 0.001 initially and the first order upwind solution method was used for momentum, turbulent kinematic viscosity, turbulent kinetic energy ' $k$ ', rate of dissipation of turbulent kinetic energy ' $\varepsilon$ ' and specific rate of dissipation of turbulent kinetic energy ' $\omega$ ' in order to get an initial solution. Once the initial solution converged, the residuals were set to  $1e-5$  and the second order upwind solution method was used. This way of obtaining the final numerical solution enabled the convergence of the results with greater ease than that by directly using smaller residuals and second order upwind solution method. The lift coefficient,  $C_l$  and the drag coefficient,  $C_d$  were obtained for different angles of attack. The angle of attack was varied by changing the components of velocity in the inlet boundary condition.

## IV. RESULTS AND DISCUSSION

### A. Velocity Magnitude Contours

The velocity magnitude contours, that were obtained for the Spalart-Allmaras, Realizable  $k-\varepsilon$  and  $k-\omega$  SST turbulence models have been illustrated in Fig. 3, Fig. 4 and Fig. 5, respectively for  $\alpha=10^\circ$ . It can be noted that the velocity magnitude contours for all the three turbulence models are in agreement with each other.

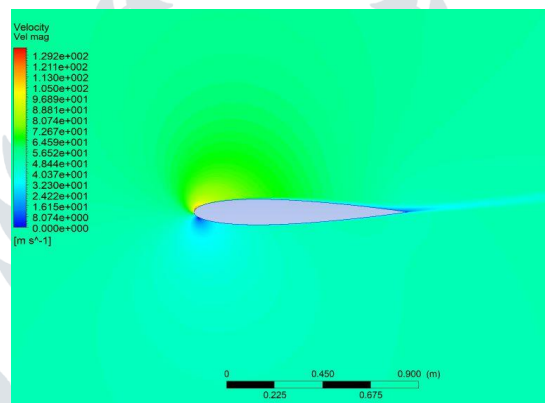


Fig. 3 Velocity magnitude contours for  $\alpha=10^\circ$  (Spalart-Allmaras)

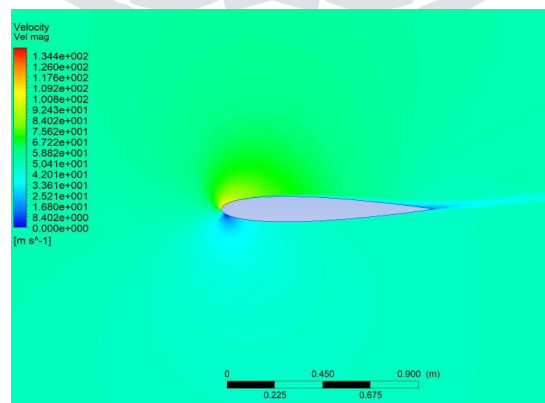


Fig. 4 Velocity magnitude contours for  $\alpha=10^\circ$  (Realizable  $k-\varepsilon$ )

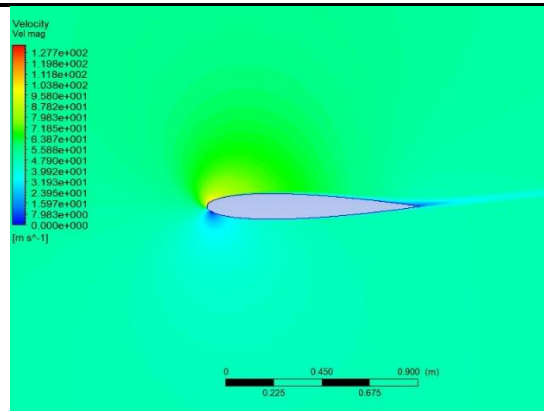


Fig. 5 Velocity magnitude contours for  $\alpha=10^\circ$  ( $k-\omega$  SST)

**B. Pressure Coefficient Curves**

The pressure coefficient curves that were obtained for the three turbulence models and their comparison with the curves obtained from [6], [7] and [8] are shown in Fig. 6, Fig. 7 and Fig. 8 respectively for  $\alpha=10^\circ$ . Since the values of pressure coefficient,  $C_p$  obtained at different points on the airfoil are nearly equal to the values of pressure coefficient on the airfoil as seen in the graph of the experimental data, it can be concluded that there is good agreement between obtained and experimental data.

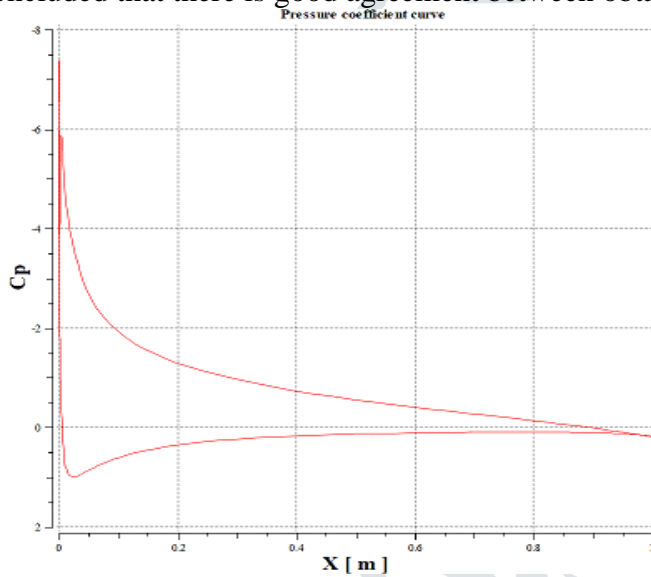


Fig. 6 Comparison of Pressure Coefficient Curves for  $\alpha=10^\circ$  (Spalart-Allmaras)

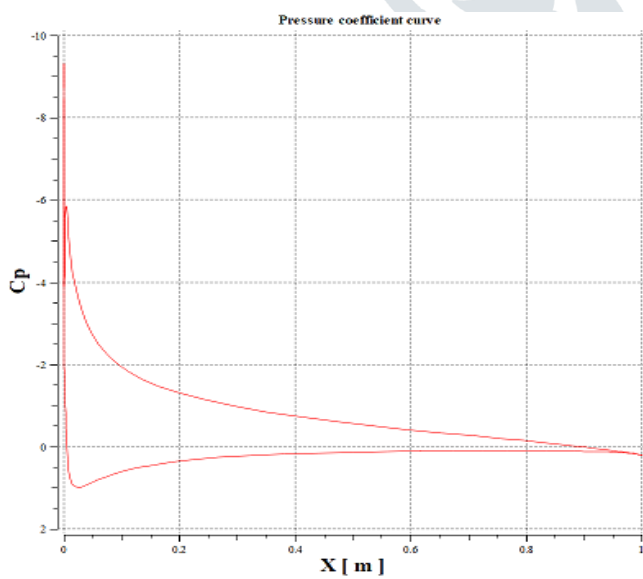
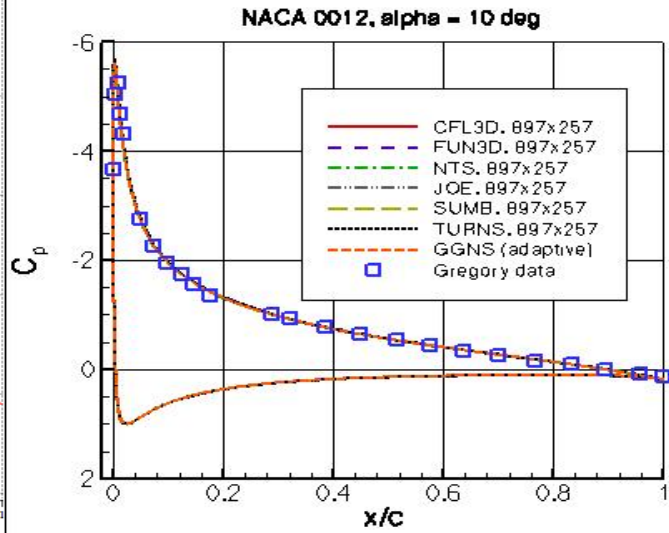
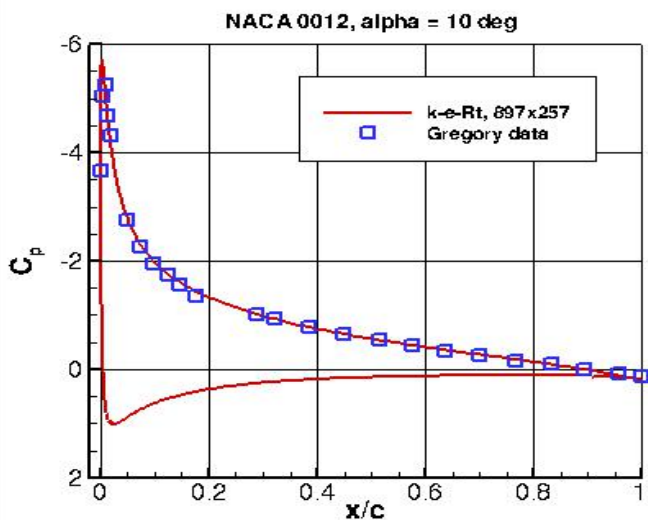
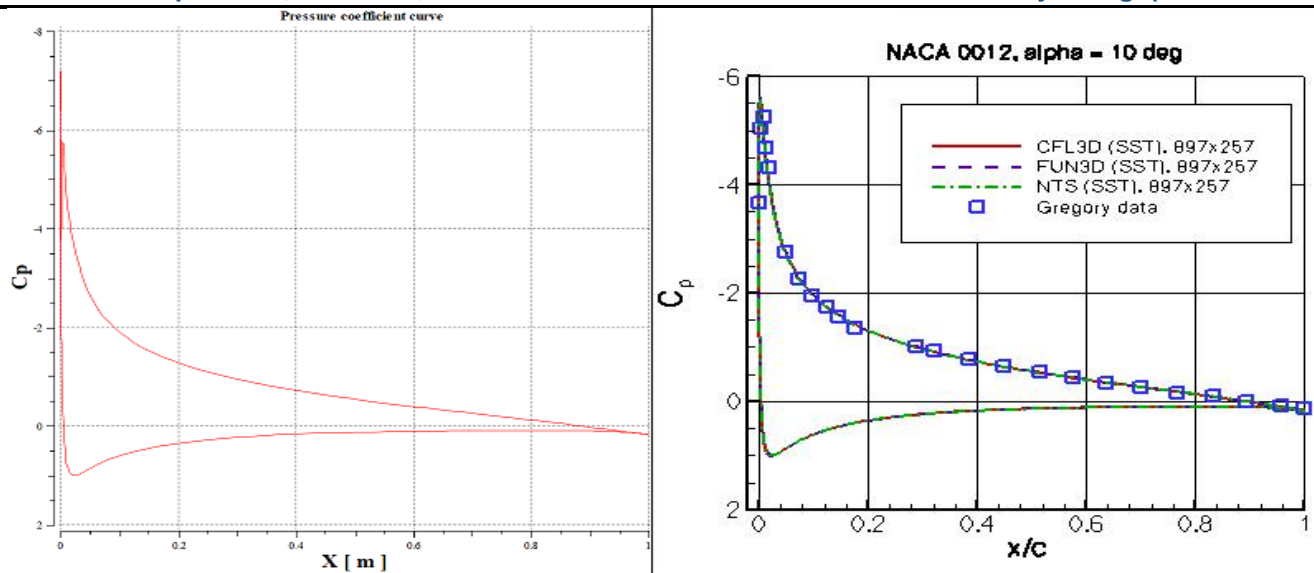


Fig. 7 Comparison of Pressure Coefficient Curves for  $\alpha=10^\circ$  (Realizable  $k-\epsilon$ )



Fig. 8 Comparison of Pressure Coefficient Curves for  $\alpha=10^\circ$  ( $k-\omega$  SST)

### C. Lift and Drag Coefficients

The lift coefficient,  $C_l$  and drag coefficient,  $C_d$  were evaluated and the results were compared with the experimental data obtained from [5], as illustrated in TABLE I and TABLE II.

TABLE I  
COMPARISON OF LIFT COEFFICIENT WITH EXPERIMENTAL DATA

Angle of Attack ( $\alpha$ )	Lift Coefficient ( $C_l$ )			
	Ladson Data	Spalart-Allmaras	Realizable $k-\epsilon$	$k-\omega$ SST
$0^\circ$	0	0	0	0
$10^\circ$	1.0707	1.066	1.0750	1.05
$15^\circ$	1.5130	1.270	1.4920	1.45

TABLE II  
COMPARISON OF DRAG COEFFICIENT WITH EXPERIMENTAL DATA

Angle of Attack ( $\alpha$ )	Drag Coefficient ( $C_d$ )			
	Ladson Data	Spalart-Allmaras	Realizable $k-\epsilon$	$k-\omega$ SST
$0^\circ$	0.0080	0.0087	0.0082	0.0081
$10^\circ$	0.0120	0.0142	0.0144	0.0140
$15^\circ$	0.0190	0.0440	0.039	0.0250

### V. CONCLUSION

The 2D CFD analysis for a NACA 0012 airfoil using different turbulence models at various angles of attack was performed. Through the velocity magnitude contours, it was observed that the turbulence models agreed well with each other. The comparison of the obtained pressure coefficient curves with the experimental pressure coefficient curves as well the comparison of the obtained lift and drag coefficients with the published experimental values indicated that the turbulence models were in agreement with the available experimental data. Hence, it was concluded that the turbulence models considered were validated.

### ACKNOWLEDGMENT

I wish to acknowledge, with a deep sense of appreciation, the guidance and encouragement received from Dr. Jayesh L. Minase. I am also thankful to my colleagues Ms. Kalyani K. Bhadekar, Mr. Sahib Bir Singh and Ms. Sai S. Aranke for their support and co-operation throughout.

### REFERENCES

- [1] Airfoil definition. [Online]. Available: <https://www.grc.nasa.gov/WWW/K-12/FoilSim/Manual/fsim001n.htm>
- [2] D.C. Eleni, T.I. Athanasios, M.P. Dionissios, "Evaluation of the turbulence models for the simulation of the flow over a National Advisory Committee for Aeronautics (NACA) 0012 airfoil," *Journal of Mechanical Engineering Research*, Vol. 4(3), March 2012, pp. 100-111.
- [3] A. Sadikin, N.A.M. Yunus, S.A.A. Hamid, A.E. Ismail, S. Salleh, S. Ahmad, M.N.A. Rahman, S. Mahzan, S.S. Ayop, "A Comparative Study of Turbulence Models on Aerodynamic Characteristics of a NACA0012 Airfoil," *International Journal of Integrated Engineering*, Vol. 10 No. 1, 2018, pp. 134-137.
- [4] T. Ahmed, M.T. Amin, S.M.R. Islam, S. Ahmed, "Computational Study of Flow Around a NACA 0012 Wing Flapped at Different Flap Angles with Varying Mach Numbers," *Global Journal of Researches in Engineering, General Engineering*, Vol. 13 Issue 4 Version 1.0, 2013.
- [5] C.L. Ladson, "Effects of Independent Variation of Mach and Reynolds Numbers on the Low-Speed Aerodynamic Characteristics of the NACA 0012 Airfoil Section," *NASA Technical Memorandum 4074*, 1988.
- [6] Information on Spalart-Allmaras model. [Online]. Available: [https://turbmodels.larc.nasa.gov/naca0012\\_val\\_sa.html](https://turbmodels.larc.nasa.gov/naca0012_val_sa.html)
- [7] Information on Realizable  $k-\epsilon$  model. [Online]. Available: [https://turbmodels.larc.nasa.gov/naca0012\\_val\\_kert.html](https://turbmodels.larc.nasa.gov/naca0012_val_kert.html)
- [8] Information on  $k-\omega$  SST model. [Online]. Available: [https://turbmodels.larc.nasa.gov/naca0012\\_val\\_sst.html](https://turbmodels.larc.nasa.gov/naca0012_val_sst.html)